

# A Selective and Ratiometric Bifunctional Fluorescent Probe for $\text{Al}^{3+}$ Ion and Proton

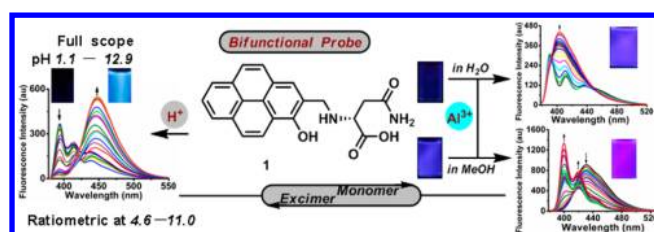
Xin Sun, Ya-Wen Wang, and Yu Peng\*

State Key Laboratory of Applied Organic Chemistry, Key Laboratory of Nonferrous Metals Chemistry and Resources Utilization of Gansu Province and College of Chemistry and Chemical Engineering, Lanzhou University, Lanzhou 730000, China

pengyu@lzu.edu.cn

Received May 20, 2012

## ABSTRACT



A new bifunctional probe based on a pyrene–amino acid conjugate for the differential response of  $\text{Al}^{3+}$  and  $\text{H}^{+}$  was demonstrated for the first time. Interestingly, two solvent-dependent sensing mechanisms for  $\text{Al}^{3+}$ , which feature a ratiometric change from excimer to monomer in  $\text{CH}_3\text{OH}$  and a turn-on response in water, are also disclosed.

Fluorescent chemosensors are widely used as powerful tools to spy on neutral and ionic species owing to their high sensitivity, selectivity, versatility, and relatively simple handling.<sup>1</sup> In particular, bifunctional probes, which refer to those based on a single host that can independently recognize two guest species with distinct spectra responses<sup>2</sup>

via the same or different channels, have already emerged and have gradually become a new research focus. This paradigm shift from selective to differential receptors<sup>3</sup> resulted from a desire to overcome difficulties such as cross-talk, a larger invasive effect, etc. encountered with the combination of several probes.<sup>4</sup> Thus, some interesting dual-analyte fluorescent probes have been successfully constructed utilizing a conventional chemosensor approach.<sup>5</sup> Alternatively, we also reported a series of bifunctional chemodosimeters based on specific chemical reactions (Scheme 1, left) and realized three types of combinations including metal ion/metal ion, anion/metal ion, and anion/anion either simultaneously or consecutively.<sup>6</sup> The design of other bifunctional probes for diverse combinations of analytes is still in high demand.

Aluminum is the most abundant metal in the Earth's crust and extensively used in modern life.<sup>7</sup> But it is neurotoxic to humans and could induce many health issues, such as Alzheimer's disease and Parkinson's disease.<sup>8</sup>

(1) (a) de Silva, A. P.; Gunaratne, H. Q. N.; Gunnlaugsson, T. A.; Huxley, J. M.; McCoy, C. P.; Rademacher, J. T.; Rice, T. E. *Chem. Rev.* **1997**, *97*, 1515. (b) Ueno, T.; Nagano, T. *Nat. Methods* **2011**, *8*, 642.

(2) The ion-pair receptors that rely on cooperative interactions among co-bound ions and a heteroditopic host do not belong to the discussion scope here; for a review, see: Kim, S.-K.; Sessler, J. L. *Chem. Soc. Rev.* **2010**, *39*, 3784.

(3) Lavigne, J. J.; Anslyn, E. V. *Angew. Chem., Int. Ed.* **2001**, *40*, 3118.

(4) These problems had been pointed out in the investigation of the bifunctional probe for  $\text{Ca}^{2+}$  and  $\text{Mg}^{2+}$ ; see: Komatsu, H.; Miki, T.; Citterio, D.; Kubota, T.; Shindo, Y.; Kitamura, Y.; Oka, K.; Suzuki, K. *J. Am. Chem. Soc.* **2005**, *127*, 10798 and references cited therein.

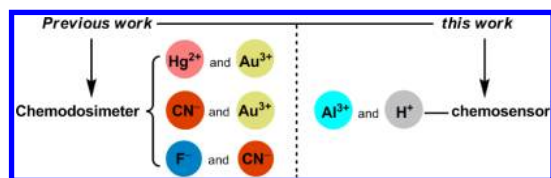
(5) (a) ( $\text{Al}^{3+}$  and  $\text{Zn}^{2+}$ ) Maity, D.; Govindaraju, T. *Chem. Commun.* **2012**, *48*, 1039. (b) ( $\text{K}^{+}$  and  $\text{F}^{-}$ ) He, X.; Yam, V. W.-W. *Org. Lett.* **2011**, *13*, 2172. (c) (Cys and Hcy) Yang, X.; Guo, Y.; Strongin, R. M. *Angew. Chem., Int. Ed.* **2011**, *50*, 10690. (d) ( $\text{Hg}^{2+}$  and saccharide) Xing, Z.; Wang, H.-C.; Cheng, Y.; James, T. D.; Zhu, C. *Chem.-Asian J.* **2011**, *6*, 3054. (e) ( $\text{Zn}^{2+}$  and  $\text{Cu}^{2+}$ ) Zhang, J. F.; Zhou, Y.; Yoon, J.; Kim, Y.; Kim, S. J.; Kim, J. S. *Org. Lett.* **2010**, *12*, 3852. (f) ( $\text{Pb}^{2+}$  and  $\text{Hg}^{2+}$ ) Hu, Z.-Q.; Lin, C.-s.; Wang, X.-M.; Ding, L.; Cui, C.-L.; Liu, S.-F.; Lu, H. Y. *Chem. Commun.* **2010**, *46*, 3765. (g) ( $\text{Cu}^{2+}$  and  $\text{Fe}^{3+}$ ) Lee, D. Y.; Singh, N.; Jang, D. O. *Tetrahedron Lett.* **2010**, *51*, 1103. (h) ( $\text{Zn}^{2+}$  and  $\text{Cd}^{2+}$ ) Xue, L.; Liu, C.; Jiang, H. *Org. Lett.* **2009**, *11*, 3454. (i) ( $\text{Hg}^{2+}$  and  $\text{Cu}^{2+}$ ) Guo, Z.; Zhu, W.; Shen, L.; Tian, H. *Angew. Chem., Int. Ed.* **2007**, *46*, 5549. (j) ( $\text{Cu}^{2+}$  and  $\text{F}^{-}$ ) Bhalla, V.; Kumar, R.; Kumar, M.; Dhir, A. *Tetrahedron* **2007**, *63*, 11153. (k) ( $\text{Cu}^{2+}$  and  $\text{F}^{-}$ ) Xu, Z.; Kim, S.; Kim, H. N.; Han, S. J.; Lee, C.; Kim, J. S.; Qian, X.; Yoon, J. *Tetrahedron Lett.* **2007**, *48*, 9151. (l) ( $\text{Pb}^{2+}$  and  $\text{F}^{-}$ ) Lee, J. Y.; Kim, S. K.; Jung, J. H.; Kim, J. S. *J. Org. Chem.* **2005**, *70*, 1463.

(6) (a) Dong, M.; Peng, Y.; Dong, Y.-M.; Tang, N.; Wang, Y.-W. *Org. Lett.* **2012**, *14*, 130. (b) Dong, Y.-M.; Peng, Y.; Dong, M.; Wang, Y.-W. *J. Org. Chem.* **2011**, *76*, 6962. (c) Dong, M.; Wang, Y.-W.; Peng, Y. *Org. Lett.* **2010**, *12*, 5310.

(7) (a) Robinson, G. H. *Chem. Eng. News* **2003**, *81* (36), 54. (b) The special issue on Aluminium: Lithosphere to Biosphere (and Back): *J. Inorg. Biochem.* **2005**, *99*, 1747.

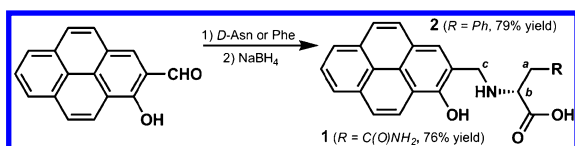
(8) (a) Perl, D. P.; Gajdusek, D. C.; Garruto, R. M.; Yanagihara, R. T.; Gibbs, C. J. *Science* **1982**, *217*, 1053. (b) Perl, D. P.; Brody, A. R. *Science* **1980**, *208*, 297.

## Scheme 1. Approaches for Designing Bifunctional Probes



To this end, the development of sensors for the facile detection of  $\text{Al}^{3+}$  is of great importance in environmental monitoring and biological assays. However, compared to other transition-metal ions, limited examples of  $\text{Al}^{3+}$  fluorescence sensors based on small molecules have been reported<sup>9</sup> and most of them worked well only in organic solvents that are difficult for practical application. In connection with our previous  $\text{H}_2\text{O}$ -tuning dual-channel fluorescence-enhanced aluminum sensor,<sup>10</sup> herein we report a highly selective fluorescent probe **1** for  $\text{Al}^{3+}$  with unique dual output modes: ratiometric in  $\text{CH}_3\text{OH}$  and turn-on in aqueous media. Meanwhile, this probe can serve as a ratiometric pH sensor with a broad range (4.6–11.0), which therefore constitutes a novel bifunctional ( $\text{Al}^{3+}/\text{H}^+$ ) probe through a chemosensor approach (Scheme 1, right). The designed **1** and control substrate **2** were easily prepared by reductive amination reactions between 1-hydroxypyrene-2-carbaldehyde<sup>11</sup> and commercially available  $\alpha$ -amino acids in high yields (see Scheme 2 and Supporting Information). Their structures were identified by  $^1\text{H}$ ,  $^{13}\text{C}$  NMR and ESI mass spectrometry (Figures S1–S6).

## Scheme 2. Synthesis of Probes



As shown in Figure 1a, the fluorescence properties of **1** were surveyed in pure  $\text{CH}_3\text{OH}$  solution. When excited at 364 nm, **1** only displays a static excimer emission band of pyrene moieties at 430 nm<sup>12</sup> which means that the excimer

is formed by an intermolecular pattern. Next, various metal ions were used to measure the selectivity of **1** in  $\text{CH}_3\text{OH}$ . With the addition of some metal ions such as  $\text{Li}^+$ ,  $\text{Na}^+$ ,  $\text{Mg}^{2+}$ ,  $\text{Ba}^{2+}$ ,  $\text{Sr}^{2+}$ ,  $\text{Zn}^{2+}$ ,  $\text{Cd}^{2+}$ , and  $\text{Mn}^{2+}$  to the solution, no significant changes of the fluorescence of **1** were observed, while  $\text{Cu}^{2+}$ ,  $\text{Fe}^{2+}$ ,  $\text{Fe}^{3+}$ ,  $\text{Pb}^{2+}$ ,  $\text{Ni}^{2+}$ ,  $\text{Hg}^{2+}$ , and  $\text{Ag}^+$  quenched the emission of **1** severely owing to the chelation enhanced fluorescent quenching (CHEQ).<sup>13</sup> Interestingly, the addition of  $\text{Al}^{3+}$  changed the emission signals of **1** remarkably and characteristic monomer emission bands (400 and 420 nm) of pyrene moieties appeared. Notably, a new shoulder peak from the dynamic excimer at  $\sim 450$  nm was also observed. Additions of  $\text{Cr}^{3+}$ ,  $\text{Co}^{2+}$ ,  $\text{Ga}^{3+}$ ,  $\text{In}^{3+}$ , and  $\text{H}^+$  show weak monomer emission, but the intensities are much smaller compared to that from  $\text{Al}^{3+}$  binding. In addition, the fluorescence color of **1** was changed from blue to purple. These unique changes revealed that **1** was highly selective for  $\text{Al}^{3+}$  in  $\text{CH}_3\text{OH}$  solution and could be a ratiometric fluorescent chemosensor for  $\text{Al}^{3+}$ .

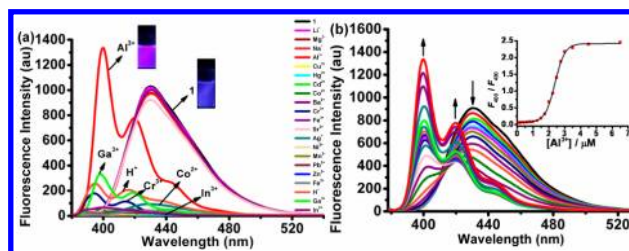


**Figure 1.** (a) Fluorescent spectra of **1** (10.0  $\mu\text{M}$ ) with various metal ions ( $\text{Li}^+$ ,  $\text{Na}^+$ ,  $\text{Mg}^{2+}$ ,  $\text{Ba}^{2+}$ ,  $\text{Sr}^{2+}$ ,  $\text{Zn}^{2+}$ ,  $\text{Cd}^{2+}$ ,  $\text{Mn}^{2+}$ ,  $\text{Cu}^{2+}$ ,  $\text{Fe}^{2+}$ ,  $\text{Fe}^{3+}$ ,  $\text{Pb}^{2+}$ ,  $\text{Ni}^{2+}$ ,  $\text{Hg}^{2+}$ ,  $\text{Ag}^+$ ,  $\text{Cr}^{3+}$ ,  $\text{Co}^{2+}$ ,  $\text{H}^+$ ,  $\text{Ga}^{3+}$ ,  $\text{In}^{3+}$ , and  $\text{Al}^{3+}$ ) (20.0 equiv) in  $\text{CH}_3\text{OH}$  (0.05% DMSO, v/v) ( $\lambda_{\text{ex}} = 364$  nm). (b) Fluorescent titrations of **1** (10.0  $\mu\text{M}$ ) with  $\text{Al}^{3+}$  (0 to 400.0  $\mu\text{M}$ ). Inset: Ratio of fluorescent intensities at 400 and 430 nm as a function of  $\text{Al}^{3+}$  concentration.

The fluorescence titration of  $\text{Al}^{3+}$  was conducted using a 10.0  $\mu\text{M}$  solution of **1** in  $\text{CH}_3\text{OH}$  (0.05% DMSO, v/v). Upon the addition of  $\text{Al}^{3+}$ , a significant increase in monomer emission at 400 and 420 nm with a concomitant decrease in excimer emission at 430 nm was observed, which is unique<sup>14</sup> compared to the usual fluorescence switch of monomer to excimer in numerous pyrene-based sensors. The fluorescent intensity ratio ( $F_{400}/F_{430}$ ) showed clear sigmoid dependence on the  $\text{Al}^{3+}$  concentration (Figure 1b, inset). This ratiometric fluorescence change<sup>15</sup> could be potentially useful for quantitative determination of  $\text{Al}^{3+}$ . A 1:1 stoichiometry complexation between **1** and

(9) (a) Jung, J. Y.; Han, S. J.; Chun, J.; Lee, C.; Yoon, J. *Dyes Pigm.* **2012**, *94*, 423. (b) Hau, F. K.-W.; He, X.; Lam, W. H.; Yam, V. W.-W. *Chem. Commun.* **2011**, *47*, 8778. (c) Lu, Y.; Huang, S.; Liu, Y.; He, S.; Zhao, L.; Zeng, X. *Org. Lett.* **2011**, *13*, 5274. (d) Maity, D.; Govindaraju, T. *Inorg. Chem.* **2010**, *49*, 7229. (e) Lee, Y. O.; Choi, Y. H.; Kim, J. S. *Bull. Korean Chem. Soc.* **2007**, *28*, 151. (f) Kim, H. J.; Kim, S. H.; Quang, D. T.; Kim, J. H.; Suh, H.-H.; Kim, J. S. *Bull. Korean Chem. Soc.* **2007**, *28*, 811. See also footnote 8 in ref 10.

(10) Ma, T.-H.; Dong, M.; Dong, Y.-M.; Wang, Y.-W.; Peng, Y. *Chem.—Eur. J.* **2010**, *16*, 10313.

(11) Prepared by the known procedure: (a) Zhou, Y.; Jung, J. Y.; Jeon, H. R.; Kim, Y.; Kim, S.-J.; Yoon, J. *Org. Lett.* **2011**, *13*, 2742. (b) Zhou, Y.; Won, J.; Lee, J. Y.; Yoon, J. *Chem. Commun.* **2011**, *47*, 1997. (c) Zhou, Y.; Wang, F.; Kim, Y.; Kim, S.-J.; Yoon, J. *Org. Lett.* **2009**, *11*, 4442.

(12) For reviews about the monomer–excimer of pyrene, see: (a) Karuppannan, S.; Chambron, J.-C. *Chem.—Asian J.* **2011**, *6*, 964. (b) Winnik, F. M. *Chem. Rev.* **1993**, *93*, 587.

(13) Chang, J. H.; Choi, Y. M.; Shin, Y.-K. *Bull. Korean Chem. Soc.* **2001**, *22*, 527.

(14) Only limited references also observed this phenomenon; see: (a) Kumar, M.; Kumar, R.; Bhalla, V. *Org. Lett.* **2011**, *13*, 366. (b) Xu, Z.; Spring, D. R.; Yoon, J. *Chem.—Asian J.* **2011**, *6*, 2114. (c) Xu, Z.; Singh, N. J.; Lim, J.; Pan, J.; Kim, H. N.; Park, S.; Kim, K. S.; Yoon, J. *J. Am. Chem. Soc.* **2009**, *131*, 15528.

(15) Only a few  $\text{Al}^{3+}$  ratiometric fluorescence sensors are known so far; see: Maity, D.; Govindaraju, T. *Chem. Commun.* **2010**, *46*, 4499 and ref 5a.

$\text{Al}^{3+}$  was obtained by using Job's plot (Figure S7). The association constant  $K$  of the complex was then calculated to be about  $10^5 \text{ M}^{-1}$  by using the emission changes at both 400 and 430 nm with Benesi–Hildbrand plots (Figures S8 and S9). Moreover, a negative-ion ESI mass spectrum provides additional evidence for the formation of a 1:1 complex of  $\mathbf{1} \cdot \text{Al}^{3+}$  (Figure S10). A peak at  $m/z$  585.0 assigned to  $[\mathbf{1} + \text{Al}(\text{III}) + 2\text{ClO}_4 - 2\text{H}]^-$  is observed. The corresponding detection limits<sup>16</sup> were determined to be 1.06 and  $0.51 \mu\text{M}$  at 400 and 430 nm, respectively (Figures S11 and S12). The fluorescent quantum yield ( $\Phi$ ) of  $\mathbf{1}$  ( $10.0 \mu\text{M}$ ) increased from 66.9% to 68.7% in the presence of  $\text{Al}^{3+}$  (40.0 equiv). To further explore the effective applications of  $\mathbf{1}$ , the competition experiments and the response time experiments were also measured. All competitive metal ions had no obvious interference with the detection of an  $\text{Al}^{3+}$  ion (Figures S13 and S14). And  $\mathbf{1}$  displayed a high sensitivity for  $\text{Al}^{3+}$  owing to the short response time (Figure S15). These results clearly indicated that  $\mathbf{1}$  is useful for selectively sensing  $\text{Al}^{3+}$  even under competition from other related metal ions, which will achieve the purpose of real-time monitoring. A blue shift change of the absorption band was observed in the UV–vis spectra of  $\mathbf{1}$  with different concentrations of  $\text{Al}^{3+}$  (Figure S16).

$^1\text{H}$  NMR studies provide additional evidence of the interaction between  $\mathbf{1}$  and  $\text{Al}^{3+}$  (Figure S17). The signals of  $\text{H}_a$ ,  $\text{H}_b$ , and  $\text{H}_c$  of  $\mathbf{1}$  were downfield shifted upon the addition of  $\text{Al}^{3+}$  (1.0 equiv), which indicated that  $-\text{OH}$ ,  $-\text{NH}$ , and  $-\text{COOH}$  or an amide group were possible binding sites for coordination with  $\text{Al}^{3+}$ . To elucidate them further, the control substrate  $\mathbf{2}$  was evaluated subsequently and high selectivity for  $\text{Al}^{3+}$  in  $\text{CH}_3\text{OH}$  was still observed (Figure S18). Accordingly, the amide group in  $\mathbf{1}$  was not the essential binding site for  $\text{Al}^{3+}$ . DFT calculations were carried out for  $\mathbf{1}$  and the  $\mathbf{1} \cdot \text{Al}^{3+}$  complex with the B3LYP/6-31 G(d) basis set using the Gaussian 03 programs. In the optimized structure of the  $\mathbf{1} \cdot \text{Al}^{3+}$  complex (Figure S19), all of pyrenoxide, secondary amine, and carboxylate oxygen of  $\mathbf{1}$  were coordinated with  $\text{Al}^{3+}$  and two perchlorate ions were counteranions. These results indicated that the formation of  $\mathbf{1} \cdot \text{Al}^{3+}$  significantly inhibited the excimer formation of  $\mathbf{1}$  in  $\text{CH}_3\text{OH}$ , which is responsible for the previously mentioned fluorescence quenching of the pyrene excimer band at 430 nm (Figure 1).

Consideration of the practical application lead to further examination of the fluorescence properties of  $\mathbf{1}$  in  $\text{H}_2\text{O}$  (0.05% DMSO, v/v) solution.<sup>17</sup> Compared to that in  $\text{CH}_3\text{OH}$ , the fluorescence intensity of free  $\mathbf{1}$  quenched significantly. But interestingly, the fluorescence spectrum of free  $\mathbf{1}$  showed three emission bands at 394, 414, and 441 nm, respectively, which were typical of pyrene monomer and excimer emission bands.<sup>12</sup> As shown in Figure 2a, compared to other metal ions examined, only  $\text{Al}^{3+}$  caused a significant fluorescence enhancement of  $\mathbf{1}$  and a new

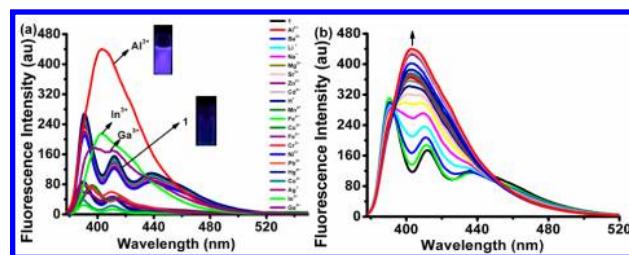


**Figure 2.** (a) Fluorescent spectra of  $\mathbf{1}$  ( $10.0 \mu\text{M}$ ) with various metal ions ( $\text{Li}^+$ ,  $\text{Na}^+$ ,  $\text{Mg}^{2+}$ ,  $\text{Ba}^{2+}$ ,  $\text{Sr}^{2+}$ ,  $\text{Zn}^{2+}$ ,  $\text{Cd}^{2+}$ ,  $\text{Mn}^{2+}$ ,  $\text{Cu}^{2+}$ ,  $\text{Fe}^{2+}$ ,  $\text{Fe}^{3+}$ ,  $\text{Pb}^{2+}$ ,  $\text{Ni}^{2+}$ ,  $\text{Hg}^{2+}$ ,  $\text{Ag}^+$ ,  $\text{Cr}^{3+}$ ,  $\text{Co}^{2+}$ ,  $\text{H}^+$ ,  $\text{Ga}^{3+}$ ,  $\text{In}^{3+}$ , and  $\text{Al}^{3+}$ ) (20.0 equiv) in  $\text{NaOAc}/\text{HOAc}$  buffer solution (0.01 M,  $\text{pH} = 4.8$ ) (0.05% DMSO, v/v) ( $\lambda_{\text{ex}} = 364 \text{ nm}$ ). (b) Fluorescent titrations of  $\mathbf{1}$  ( $10.0 \mu\text{M}$ ) with  $\text{Al}^{3+}$  (0 to  $400.0 \mu\text{M}$ ).

emission band at 405 nm appeared. The pH effect on the fluorescence intensity was shown in Figures S20 and S29. The response of  $\mathbf{1}$  with the  $\text{Al}^{3+}$  system exhibited a constant between  $\text{pH}$  4.4 and 6.0. In this pH range, only a small change was observed in the free  $\mathbf{1}$  system. In subsequent experiments, a  $\text{pH}$  4.8 solution was used as an ideal medium. The addition of  $\text{Al}^{3+}$  resulted a 3.6-fold fluorescence enhancement at 405 nm (Figure 2b), which denoted chelation-enhanced fluorescence (CHEF).<sup>18</sup> The titration experiment shows two distinct isoemissive points at 393 and 450 nm with an intensity decrease in the two bands at about 390 and 460 nm, which is responsible for breaking the monomer–excimer equilibrium of  $\mathbf{1}$  in  $\text{H}_2\text{O}$  solution after the formation of the  $\mathbf{1} \cdot \text{Al}^{3+}$  complex.<sup>12</sup> The fluorescent quantum yield ( $\Phi$ ) of  $\mathbf{1}$  ( $10.0 \mu\text{M}$ ) increased from 43.1% to 45.6% in the presence of  $\text{Al}^{3+}$  (40 equiv). Moreover, a 1:1 stoichiometry complexation between  $\mathbf{1}$  and  $\text{Al}^{3+}$  was also obtained similarly (Figures S21 and S22). The association constant was calculated to be  $1.23 \times 10^5 \text{ M}^{-1}$ , and the corresponding detection limit was found to be  $0.49 \mu\text{M}$  (Figure S23), which is lower than the US EPA and FDA guideline of  $7.41 \mu\text{M}$   $\text{Al}^{3+}$  for bottled drinking water.  $^1\text{H}$  NMR studies were also carried out (Figure S24). All competitive metal ions had no obvious interference with the detection of  $\text{Al}^{3+}$  ion (Figure S25). And  $\mathbf{1}$  still displayed a short response time for sensing  $\text{Al}^{3+}$  (Figure S26). In addition, the dark blue fluorescence of  $\mathbf{1}$  also changed to blue-violet. In the UV–vis spectra of  $\mathbf{1}$  in  $\text{H}_2\text{O}$ , the absorption peak at 344 nm decreased and the peak at 386 nm increased upon the addition of  $\text{Al}^{3+}$ , and slight red shifts were observed at the absorption band (Figure S27).

Then, we studied the bioimaging application of  $\mathbf{1}$  for sensing  $\text{Al}^{3+}$  ions in living cells. HeLa cells were incubated with  $\mathbf{1}$  ( $10.0 \mu\text{M}$ ) for 30 min at  $37^\circ\text{C}$ , and the cells showed weak fluorescence (Figure 3b). Once the treated cells were incubated with  $\text{Al}^{3+}$  ( $200.0 \mu\text{M}$ ) in the culture medium for 30 min at  $37^\circ\text{C}$ , a significant increase of the fluorescence

(16) For the calculation method employed, see: Lin, W.; Yuan, L.; Cao, Z.; Feng, Y.; Long, L. *Chem.—Eur. J.* **2009**, *15*, 5096.

(17) This nearly pure water media for  $\text{Al}^{3+}$  fluorescence sensing is very rare; for more details, see ref 9.

(18) (a) Kim, J. S.; Noh, K. H.; Lee, S. H.; Kim, S. K.; Kim, S. K.; Yoon, J. J. *Org. Chem.* **2003**, *68*, 597. (b) Chae, M.-Y.; Yoon, J.; Czarnik, A. W. *J. Mol. Recognit.* **1996**, *9*, 297. (c) Akkaya, E. U.; Huston, M. E.; Czarnik, A. W. *J. Am. Chem. Soc.* **1990**, *112*, 3590.



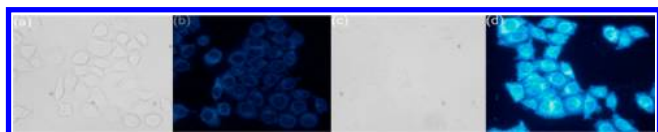


**Figure 3.** Images of HeLa cells: (a) bright field image of HeLa cells incubated with **1** (10.0  $\mu\text{M}$ ); (b) fluorescence image of (a); (c) bright field image of HeLa cells incubated with **1** (10.0  $\mu\text{M}$ ) for 30 min, and then further incubation with  $\text{Al}^{3+}$  (200.0  $\mu\text{M}$ ) for 30 min at 37  $^{\circ}\text{C}$ ; (d) fluorescence image of (c).

from the intracellular area was observed (Figure 3d). These results suggest that **1** is cell membrane permeable and could be used for detecting  $\text{Al}^{3+}$  within living cells.

Protons play critical roles in many cellular events<sup>19</sup> such as cell growth apoptosis, calcium regulation, endocytosis, etc. Thus, protons have become one of the most important sensing targets<sup>20</sup> among the interesting species in vivo. The other aspect of **1** as a bifunctional probe was demonstrated in the following pH sensing investigation. With the increase of pH from 1.1 to 12.9, the fluorescence spectra of **1** exhibited a decrease of monomer emission bands with a concomitant increase of excimer emission bands (Figure 4a), which is just the reverse compared to the  $\text{Al}^{3+}$  titration process (excimer $\downarrow$ , monomer $\uparrow$ ) in  $\text{CH}_3\text{OH}$  (Figure 1b). A red shift change of the absorption band was also observed in the UV-vis spectra of **1** with different pH values (Figure S28). This broad pH response could be attributed to the protonation process of **1**.<sup>21</sup> At a high pH value, the amino group might form a strong hydrogen bond with the phenoxide group, which could lead to the coplanarity of pyrene and the binding sites. Therefore, the excimer band predominates due

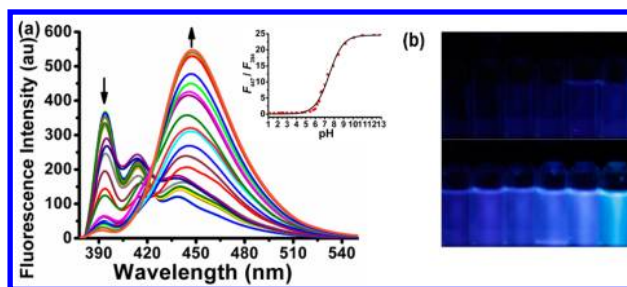


**Figure 4.** (a) Fluorescent spectra of **1** (10.0  $\mu\text{M}$ ) in various pH values (1.1, 1.6, 2.1, 2.4, 2.6, 3.0, 3.5, 4.0, 4.6, 4.9, 5.5, 5.8, 6.0, 6.2, 6.4, 6.6, 6.7, 7.0, 7.3, 7.9, 8.5, 9.2, 10.0, 11.0, 12.2, 12.9). Inset: Ratio of fluorescent intensities at 447 and 394 nm as a function of pH. (b) Fluorescence color changes of **1**. Top to bottom: pH = 2.1, 3.0, 4.0, 4.9, 6.0, 7.0, 7.9, 9.2, 10.0, 11.0, 12.2, 12.9.

to a strong  $\pi$ – $\pi$  interaction. At a low pH value, the amino group of **1** must be protonated resulting in a more flexible conformation. So the monomers as the main peaks and excimer band are all observed. Moreover, the ratios of the emission intensities at 447 and 394 nm ( $F_{447}/F_{394}$ ) showed a sigmoid dependence on the proton concentration within the broad range pH 4.6–11.0<sup>22</sup> (Figure 4a, inset). The enhancement factor was determined as being prominently 49.8-fold which means this probe could precisely respond to minor pH fluctuations. Using the Henderson–Hasselbalch equation, the  $\text{p}K_{\text{a}}$  of **1** was calculated to be 6.68 ( $\pm 0.03$ )<sup>23</sup> which is close to neutral pH and suitable for studying biological systems (Figure S29). The fluorescent quantum yields of **1** at pH 1.1, 6.7, and 12.9 are 45.2%, 53.7%, and 65.8%, respectively. With pH variation, the fluorescence color of **1** changed from dark blue to light blue that could be observed by the naked eye (Figure 4b), indicating that **1** could be used as a ratiometric pH fluorescent sensor.

In summary, an unprecedented bifunctional probe for recognition of the aluminum ion and protons has been demonstrated, which provided another example for this rare combination (metal ion/proton).<sup>21,24</sup> Utilizing other easily available pyrene–amino acid conjugates, extension of the present work to combinations of diverse species is ongoing and will be reported in due course.

**Acknowledgment.** We thank Mr. Ming Dong for performing computational studies. This work was supported by NSFC (Nos. 21001058 and 21172096), the Scientific Research Foundation for the Returned Overseas Chinese Scholars, the Fundamental Research Funds for the Central Universities (Izujbky-2012-57), and the “111” Project of MoE.

**Supporting Information Available.** Experimental procedures, spectral data, and copies of  $^1\text{H}/^{13}\text{C}$  NMR and MS. This material is available free of charge via the Internet at <http://pubs.acs.org>.

The authors declare no competing financial interest.

(19) (a) Gottlieb, R. A.; Nordberg, J.; Skowronski, E.; Babior, B. M. *Proc. Natl. Acad. Sci. U.S.A.* **1996**, *93*, 654. (b) Golovina, V. A.; Blaustein, M. P. *Science* **1997**, *275*, 1643. (c) Yuli, I.; Oplatka, A. *Science* **1987**, *235*, 340. (d) Paradiso, A. M.; Tsien, R. Y.; Machen, T. E. *Nature* **1987**, *325*, 447.

(20) Han, J.; Burgess, K. *Chem. Rev.* **2010**, *110*, 2709.

(21) For a related discussion, see: Tolosa, J.; Bryant, J. J.; Solntsev, K. M.; Brödner, K.; Tolbert, L. M.; Bunz, U. H. F. *Chem.—Eur. J.* **2011**, *17*, 13726.

(22) For other ratiometric pH sensors based on small molecules, see: (a) (pH 3.0–8.6) Lin, W.; Yuan, L.; Cao, Z.; Feng, Y.; Song, J. *Angew. Chem., Int. Ed.* **2010**, *49*, 375. (b) (pH 4.0–6.5) Han, J.; Loudet, A.; Barhoumi, R.; Burghardt, R. C.; Burgess, K. *J. Am. Chem. Soc.* **2009**, *131*, 1642. (c) (pH 6.7–7.9) Tang, B.; Yu, F.; Li, P.; Tong, L.; Duan, X.; Xie, T.; Wang, X. *J. Am. Chem. Soc.* **2009**, *131*, 3016. (d) (pH 3.0–8.0) Charrierq, S.; Ruel, O.; Baudin, J.-B.; Alcor, D.; Allemand, J.-F.; Meglio, A.; Jullien, L. *Angew. Chem., Int. Ed.* **2004**, *43*, 4785.

(23) For a recent report with similar  $\text{p}K_{\text{a}}$  calculated through  $-\log[(F_{\text{max}} - F)/(F - F_{\text{min}})] = \text{pH} - \text{p}K_{\text{a}}$  where  $F$  is fluorescence intensity at a fixed wavelength, see: Saha, U. C.; Dhara, K.; Chattopadhyay, B.; Mandal, S. K.; Mandal, S.; Sen, S.; Mukherjee, M.; van Smaalen, S.; Chattopadhyay, P. *Org. Lett.* **2011**, *13*, 4510.

(24) Other cases did not demonstrate specificity to some metal ions or serve as a molecular logic-gate instead; see: (a) Tolosa, J.; Zuccherro, A. J.; Bunz, U. H. F. *J. Am. Chem. Soc.* **2008**, *130*, 6498. (b) Li, Y. Q.; Bricks, J. L.; Resch-Genger, U.; Spieles, M.; Rettig, W. *J. Phys. Chem. A* **2006**, *110*, 10972. (c) Kou, S.; Lee, H. N.; van Noort, D.; Swamy, K. M. K.; Kim, S. H.; Soh, J. H.; Lee, K.-M.; Nam, S.-W.; Yoon, J.; Park, S. *Angew. Chem., Int. Ed.* **2008**, *47*, 872. (d) Magri, D. C.; Brown, G. J.; McClean, G. D.; de Silva, A. P. *J. Am. Chem. Soc.* **2006**, *128*, 4950. (e) de Silva, A. P.; Gunaratne, H. Q. N.; McCoy, C. P. *Nature* **1993**, *364*, 42.